Journal of Hydrology, 79 (1985) 333—358
Elsevier Science Publishers B.V., Amsterdam — Printed in The Netherlands

[3]

ON THE THEORY OF TRACER EXPERIMENTS IN FISSURED ROCKS WITH A POROUS MATRIX

P. MAŁOSZEWSKI and A. ZUBER

Institute of Nuclear Physics, Radzikowskiego 152, PL 31-342 Cracow 23 (Poland)

(Accepted for publication March 21, 1985)

ABSTRACT

Małoszewski, P. and Zuber, A., 1985. On the theory of tracer experiments in fissured rocks with a porous matrix. J. Hydrol., 79: 333—358.

A model of parallel fractures, having equal spacing and width, has been applied to tracer movement in fissured rocks with a porous matrix. The exact solution has been obtained for instantaneous injection. Graphical presentations demonstrate the applicability and the limitations of particular approximations. In short-term experiments the single fracture approximation works well because the tracer has not penetrated the matrix deeply enough to be influenced by the adjacent fractures. In high matrix porosity, diffusion into the matrix is dominant and the model may be simplified by neglecting the influence of dispersivity. In low matrix porosity, a dispersion model with no diffusion into the matrix may often yield approximately the mean transit time of water. By contrast, in long-term tracer experiments, the tracer appears to exploit the whole water volume, i.e. both the mobile fissure volume and the stagnant micropore volume. The tracer curve yields the mean transit time of tracer, which is related to the mean transit time of water by the retardation factor. This factor is expressed approximately by the ratio of total porosity to fissure porosity, provided the tracer is non-adsorbable. For adsorbable tracers the microporosity acts as a strong sink due to the large adsorption surface. This fact is most probably the cause of the discrepancies observed between ^{14}C ages in carbonate aquifers and the stable isotope shift expected from the climate change at the end of the last glaciation. It is also shown that the ^{14}C exchange in carbonate rocks may yield ^{14}C ages orders of magnitude too high in comparison with conventional flow data. Examples of the interpretation of artificial tracer experiments demonstrate that the model developed works surprisingly well.

INTRODUCTION

The movement of solutes in fissured rocks with a porous matrix has attracted a lot of attention in recent years. Most authors concentrated on the movement of continuously injected pollutants (Grisak and Pickens, 1980, 1981; Grisak et al., 1980; Neretnieks, 1980; Neretnieks et al., 1982; Rasmuson and Neretnieks, 1981; Sudicky and Frind, 1981, 1982; Tang et al., 1981). Foster (1975) showed that the anomalously low tritium content in the English Chalk was caused by its diffusion into the porous

0022-1694/85/$03.30

matrix during infiltration through the unsaturated zone. Freeze and Cherry (1979) supported this idea and reviewed early works on the subject. Neretnieks (1981) showed that the diffusion of tracer into the porous matrix leads to false ^{14}C ages. Glueckauf (1981) dealt with artificial tracer experiments by applying a theoretical plate model, physically identical to the model adopted here, i.e., to the dispersion equation in fissures coupled with the molecular diffusion equation in the matrix. However, Glueckauf's solution is limited to a single-fracture approximation and the numerical results in some cases contradict the physical expectations and the more exact results obtained here. Black and Kipp (1983) replaced the diffusion equation by a mass-transfer equation similar to that in the dead-end pore model. The model yields curves which fit the experimental data well, which is hardly surprising in view of the large number of adjustable parameters. However, the extremely high values of fissure porosities (or large pore porosities) presented in Black and Kipp's tables II and III are unrealistic. Sudicky and Frind (1982) obtained an analytical solution in the case of a continuous injection for a model of parallel fissures equally spaced. Małoszewski and Zuber (1983) found an analytical solution for an instantaneous injection, although their numerical considerations are limited to long-term experiments. A generalized version of this model takes into account the reversible adsorption isotherm. Numerical results for short-term experiments are given and shown to be compatible with a simplified model for a single fracture.

The model shows that the adsorption of ^{14}C in a porous matrix may be responsible for the discrepancy between the ^{14}C ages and the change in the isotopic composition of water caused by the climatic changes at the end of the last glaciation.

It should be mentioned that further improvement of the mathematical modelling of transport in fissured media may be achieved by following Barker (1982, 1985) who used the numerical inversion of the Laplace transform, and introduced block-geometry functions which represent the matrix geometry in a generalized equation reduced to a standard form.

THE MODEL AND ANALYTICAL SOLUTIONS

The dual-porosity medium is approximated by a semi-infinite system of identical parallel fissures equally spaced in a porous matrix. The tracer is instaneously injected into water entering the fissures, and is transported along the fissures by groundwater flow. The flow rate in fissures is assumed to be fast enough for transport in the axial direction through the porous matrix to be neglected. The tracer distribution across the fissure width is assumed to be constant due to sufficient transverse dispersion and diffusion. The movement of the tracer in the porous matrix is governed by molecular diffusion and reversible adsorption with a linear adsorption isotherm. The

adsorption in the fissures is negligible because of the small surface available. Using these assumptions the following equations for the mass balance in the fissures and in the matrix can be written down:

$$\frac{\partial C_f}{\partial t} + v\frac{\partial C_f}{\partial x} - D\frac{\partial^2 C_f}{\partial x^2} + \lambda C_f - \frac{n_p D_p}{b}\frac{\partial C_p}{\partial y}\bigg|_{y=b} = 0 \tag{1}$$

$$\frac{n_p \partial C_p}{\partial t} + (1-n_p)\rho\frac{\partial C_s}{\partial t} - n_p D_p\frac{\partial^2 C_p}{\partial y^2} + \lambda[n_p C_p + (1-n_p)\rho C_s] = 0 \tag{2}$$

where C_f and C_p are the tracer concentrations in water in the fissures and in the matrix respectively, C_s is the tracer concentration in the solid material of the matrix, v is the mean water velocity in fissures, x is the spatial coordinate taken in the direction of flow, y is the spatial coordinate perpendicular to the fissure extension, t is the time variable, λ is the radioactive decay constant, n_p is the matrix porosity, ρ is the density of matrix material, D_p is the molecular diffusion coefficient in the porous matrix, D is the dispersion coefficient in the fissures, b is the half-fissure aperture, and L is the fissure spacing (see eqn. (4.3) below). Assuming the linear adsorption isotherm and an instantaneous equilibrium between the solid and liquid phases, the distribution coefficient, $k_d = C_s/C_p$, can be inserted into eqn. (2) yielding:

$$\frac{\partial C_p}{\partial t} - \frac{n_p D_p}{n_p + (1-n_p)\rho k_d}\frac{\partial^2 C_p}{\partial y^2} + \lambda C_p = 0 \tag{2.1}$$

Equation (1) describes the convective and dispersive transport in fissures, whereas eqn. (2), or (2.1), describes the diffusive transport in the matrix perpendicular to the fissures. The following initial and boundary conditions are used to solve these equations for instantaneous injection:

$$C_f(x, 0) = 0 \tag{3.1}$$

$$C_f(0, t) = A_o\delta(t) \tag{3.2}$$

$$C_f(\infty, t) = 0 \tag{3.3}$$

$$C_p(y, x, 0) = 0 \tag{4.1}$$

$$C_p(b, x, t) = C_f(x, t) \tag{4.2}$$

$$\frac{\partial C_p}{\partial y}\left(\frac{L}{2}\right), x, t = 0 \tag{4.3}$$

where $A_o = A/(n_f v S)$, A being the injected mass or activity, S the cross-section area perpendicular to the flow, and n_f the fissure porosity ($n_f = 2b/L$).

Solutions to eqns. (1) and (2) with conditions (3) and (4), but without adsorption, i.e. for $k_d = 0$, were derived by Małoszewski and Zuber (1983). Similarly, one can easily obtain the solutions for $k_d \neq 0$. They are as follows:

$$\frac{C_f(t)}{A_o} = \frac{2}{\pi^{3/2}} \exp\left(\frac{Pe}{2}\right) \int_w^\infty \exp\left[-\xi^2 - \left(\frac{Pe}{4\xi}\right)^2\right] \left[\int_0^\infty \epsilon \exp(-\epsilon_1)\cos(\epsilon_2)d\epsilon\right] d\xi \tag{5}$$

where:

$$w = 0.5(Pe\, t_o/t)^{1/2} \tag{6}$$

$$\epsilon_1 = \frac{Pe\, t_o a}{4} \frac{\epsilon}{\xi^2} \left[\frac{\sinh(\delta\epsilon) - \sin(\delta\epsilon)}{\cosh(\delta\epsilon) + \cos(\delta\epsilon)}\right] \tag{7}$$

and:

$$\epsilon_2 = \frac{\epsilon^2}{2}\left(t - 0.25Pe\frac{t_o}{\xi^2}\right) - Pe\, t_o \frac{a\epsilon}{4\xi^2}\left[\frac{\sinh(\delta\epsilon) + \sin(\delta\epsilon)}{\cosh(\delta\epsilon) + \cos(\delta\epsilon)}\right] \tag{8}$$

ξ and ϵ being the integration variables. The parameters are expressed as follows:

$$Pe = vx/D \tag{9}$$

is the Pêclet number, or the reciprocal of the dispersion parameter, constant for a given x and pure hydrodynamical dispersion;

$$t_o = x/v = V_f/Q \tag{10}$$

is the mean transit time of water (V_f is the volume of fissures i.e. mobile water volume, and Q is the volumetric flow rate through the system);

$$\delta = (L/2 - b)\sqrt{R_a}/\sqrt{D_p} \tag{11}$$

and:

$$a = n_p\sqrt{R_a D_p}/(2b) \tag{12}$$

where:

$$R_a = 1 + (n_p^{-1} - 1)\rho k_d \tag{13}$$

is the commonly applied retardation factor for reversible adsorption.

Equations (5—8) are the same as those given by Małoszewski and Zuber (1983) for the case of $R_a = 1$. Thus, the solutions for the reversible adsorption in the matrix differ from those without adsorption by the $\sqrt{R_a}$ factor in eqns. (11) and (12).

For a single fracture, instead of eqn. (4.3) the following condition is used:

$$\lim_{y \to \infty} C_p = 0 \tag{14}$$

The solution for the dispersion model is then:

$$\frac{C_f(t)V_f}{A} = \frac{2a\, t_o}{\pi} \int_w^\infty u(t-u)^{-3/2} \exp\left[-\xi^2\left(1 + \frac{u}{t_o}\right)^2 - \frac{a^2u^2}{t-u}\right] d\xi \tag{15}$$

where:

$$u = \frac{Pe\, t_o}{4\xi^2} \tag{16}$$

For $D = 0$ the solution is:

$$C_f(t)\, t_o / A_o = C_f V_f / A$$
$$= a(t_o/\pi)^{1/2}(t/t_o - 1)^{-3/2} \exp[-a^2 t_o/(t/t_o - 1)] \tag{17}$$

Inspection of the above formulae leads to the conclusion that the number of parameters may be reduced to four for eqn. (5) (t_o, Pe, a, δ), to three for eqn. (15) (t_o, Pe, a), and to two for eqn. (17) (t_o, a).

THE MEAN TRANSIT TIME OF TRACER

The mean transit time of tracer is defined as:

$$\bar{t}_t = \int_0^\infty t C_f(t)\, dt \Big/ \int_0^\infty C_f(t)\, dt \tag{18}$$

where C_f is here the concentration resulting from an instantaneous injection. The method of moments, applied to the Laplace transform of C_f yields for $\lambda = 0$ and $k_d = 0$ (Małoszewski and Zuber, 1983):

$$\bar{t}_t = [1 + n_p(L - 2b)/2b]\, t_o = (1 + 2a\delta)\, t_o = R_p\, t_o \tag{19}$$

where:

$$R_p = 1 + n_p(L - 2b)/2b = 1 + (n_p/n_f) - n_p \tag{20}$$

may be defined as the retardation factor due to diffusion into the porous matrix. To a good approximation, the R_p factor is:

$$R_p \cong 1 + n_p/n_f \tag{21}$$

this is the total open porosity divided by the fissure porosity. For example, if both n_p and n_f are equal to 0.03, eqn. (21) differs from (20) by 1.5%.

In the case of an adsorbable tracer:

$$\bar{t}_t = R t_o = (1 + 2a\delta) t_o \cong [1 + (n_p/n_f) R_a]\, t_o \tag{22}$$

where R is the total retardation factor.

Equation (19), expressed in terms of velocity, v and v_t, shows that the tracer velocity v_t is not related to distance from the injection point, thus contrary to the hypothesis of Neretnieks (1980), it does not depend on the depth of penetration. On the other hand, as shown in the next section, the mean transit time of tracer and, consequently, the tracer velocity is not measurable by the method of moments [eqn. (18)] in short-term experiments.

For a single fracture approximation $\delta \to \infty$ and consequently both $R \to \infty$ and $\bar{t}_t \to \infty$, the method of moments is then inapplicable both in theory and in practice.

TRACER CONCENTRATION CURVES FOR INSTANTANEOUS INJECTION

Normalized tracer concentration curves for short transit times are shown in Figs. 1—4. Such normalized concentration also expresses the so-called weighting function, $g(t)$ (transit-time distribution of the tracer), which determines the tracer curve from the convolution integral for an arbitrary injection. The time scale is normalized to the mean transit time of water, t_o. However, such normalization, though convenient for graphical presentation of different concentration curves, does not eliminate the influence of ordinary time in the case of delayed tracer curves.

Figure 1 shows that the dispersion version of the single-fracture model (DM—SF) yields practically the same concentration curves as the dispersion model in a system of parallel fractures (DM—PF), if the mean transit time of water is sufficiently short, i.e. of the order of one month. This implies that in short-term experiments the tracer has no time to diffuse deep enough into the matrix to be affected by adjacent fissures. For short-term experiments this fact allows omission of one fitting parameter (δ).

In very short-time tracer experiments (of the order of tens of hours) the tracer curves (Fig. 2) approximate to the curves given by the ordinary dispersion model, without a porous matrix. Fitting of an adequate ordinary dispersion model may yield flow parameters (t_o and consequently v) with adequate accuracy. However, the method of moments will yield erroneous results. Consider the parallel-fracture model in Fig. 1, eqn. (22) yields $\bar{t}_t = 1.97t_o$, i.e. the mean transit time of the tracer is nearly twice the mean transit time of the water. This results from a long-tail effect, which is not obvious in the figure. In the examples in Fig. 2, the theoretical mean transit

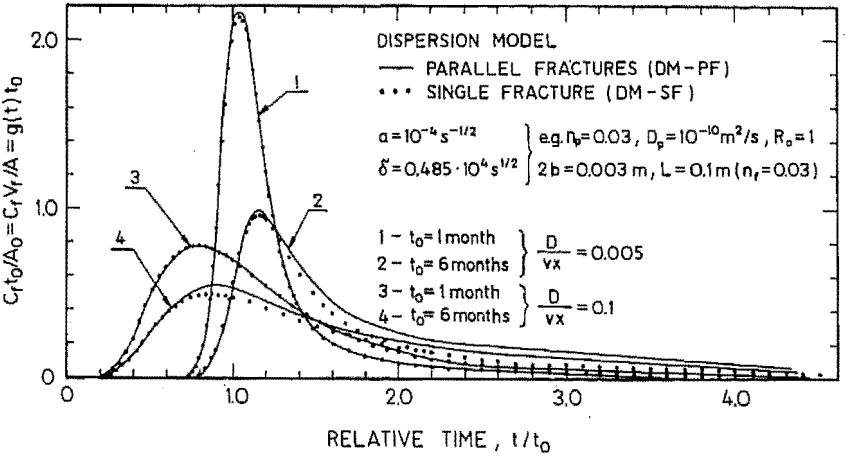

Fig. 1. Examples of concentration curves resulting from an instantaneous injection for the dispersion model of parallel fractures [eqn. (5)] and single fracture [eqn. (15)] in the case of intermediate-term experiments.

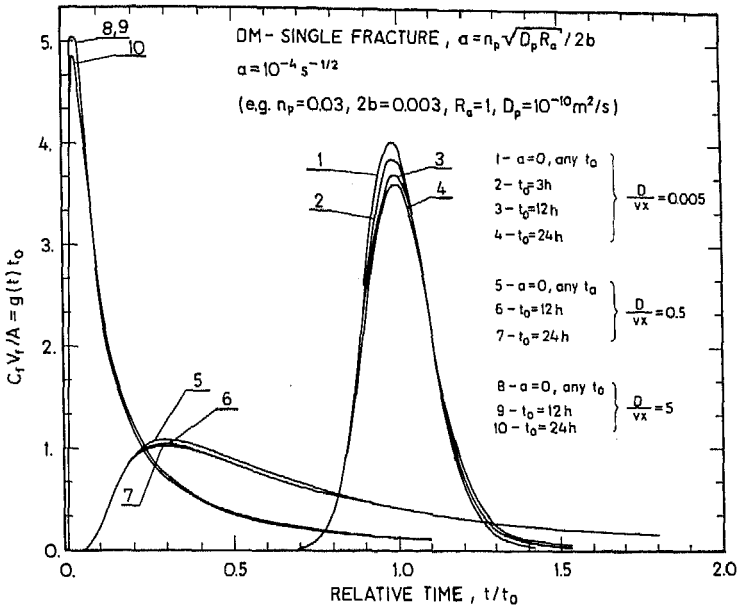

Fig. 2. Examples of concentration curves for the dispersion model of single fracture [eqn. (15)] as compared to the ordinary dispersion model [eqn. (23)], i.e. when $a = 0$ in the case of short-term experiments.

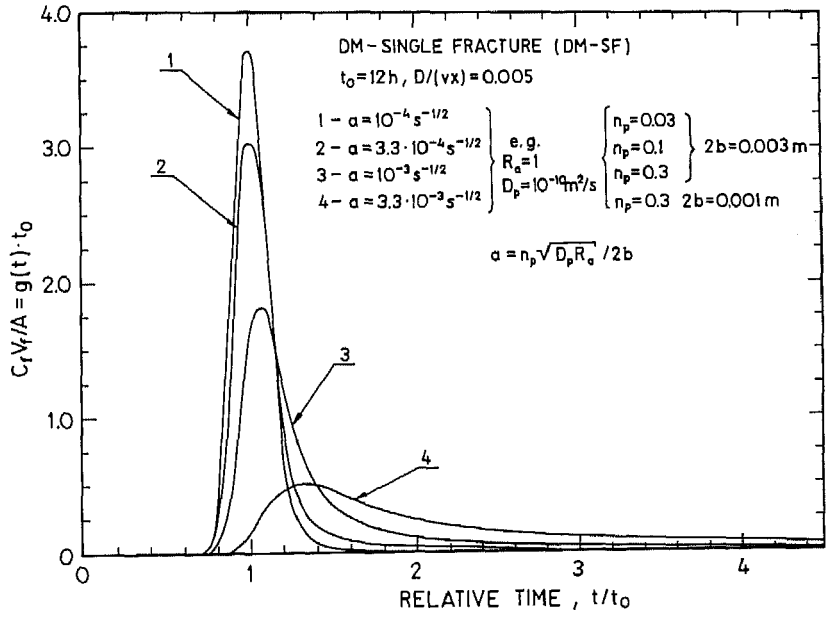

Fig. 3. The influence of increasing a-value in the case of the dispersion model of single fracture [eqn. (15)] in short-term experiments.

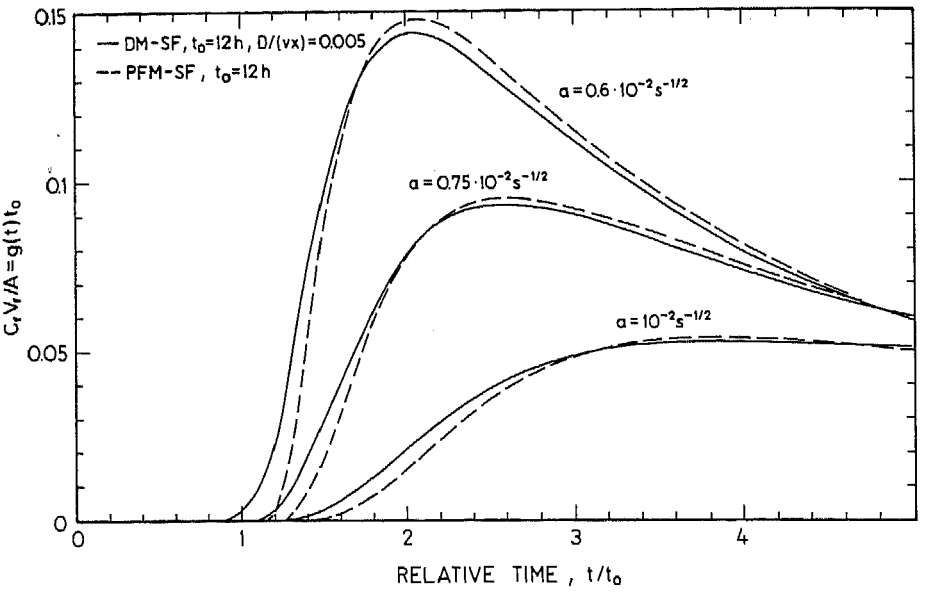

Fig. 4. Examples demonstrating that when a-value is sufficiently high the piston flow model of single fracture [eqn. (17)] is a good approximation of the dispersion model [eqn. (15)] in short-term experiments.

time of tracer is not defined because part of the tracer will be lost in the matrix by diffusion. The experimenter may calculate $\bar{t}_t$ from his experimental curve by utilizing eqn. (18), but the result will depend on the accuracy of the tail measurement and on the amount of injected tracer. The higher the accuracy or the amount of tracer, the greater the value of $\bar{t}_t$ that will be obtained. Thus, the system is not linear when the method of moments [eqn. (18)] is utilized for the interpretation. The same is true in the case of parallel fissures, although theoretically the first moment exists. A strong tailing effect makes experimental determination of the mean transit time of tracer very difficult.

The ordinary dispersion model utilized within this work is that derived by Lenda and Zuber (1970), discussed in detail by Kreft and Zuber (1978), and followed by Małoszewski and Zuber (1982). In a form normalized to t_o it reads:

$$\frac{C_f V_f}{A} = \left[\frac{Pe}{4\pi(t/t_o)^3}\right]^{1/2} \exp\left[-\frac{(1-t/t_o)^2 Pe}{4(t/t_o)}\right] \tag{23}$$

Figures 3 and 4 demonstrate that, even for very short-term experiments, the ordinary dispersion model becomes inapplicable in the case of narrow fissures and high matrix porosity, i.e. for high values of the a-parameter. For the t_o values in Fig. 3, a-parameter values up to $3\cdot10^{-4}$ $s^{-1/2}$ would yield curves interpretable by the ordinary dispersion model, DM (adjusting

the concentration scale and rejecting the tail). Above that value of a, the fitting of the ordinary DM will yield erroneous values for the parameters. Figure 4 also shows that in short-term experiments with a high value of the a-parameter, a two-parameter model of eqn. (17) is a good approximation.

In summary, for short-term experiments, if a is low, the experimenter may determine t_o from the two-parameter ordinary dispersion model [eqn. (23)], when a is high both t_o and a can be found from another simple two-parameter model [eqn. (17)]. The three-parameter dispersion model of a single fracture, DM—SF [eqn. (15)], is generally applicable.

In contrast for long-term experiments and high values of a-parameter the tracer curves (Fig. 5) tend to be more symmetrically distributed around the mean transit time of the tracer, $\bar{t}_t$. They are also interpretable by the ordinary dispersion model DM with apparent $D/(vx)$ values (Małoszewski and Zuber, 1983). However, according to eqn. (22), t_o in eqn. (23) must be replaced by $\bar{t}_t$, and for theoretical comparison the concentration scales are transformed by eqn. (24), which results from the normalization procedure:

$$\left(\frac{C_f V_t}{A}\right)_{\text{ordinary DM}} = \left(R\,\frac{C_f V_f}{A}\right)_{\text{DM—PF}} \tag{24}$$

where V_t is the total volume of water in the system. In Fig. 5 the comparison is obtained by dividing eqn. (24) by R. Other ordinary dispersion models

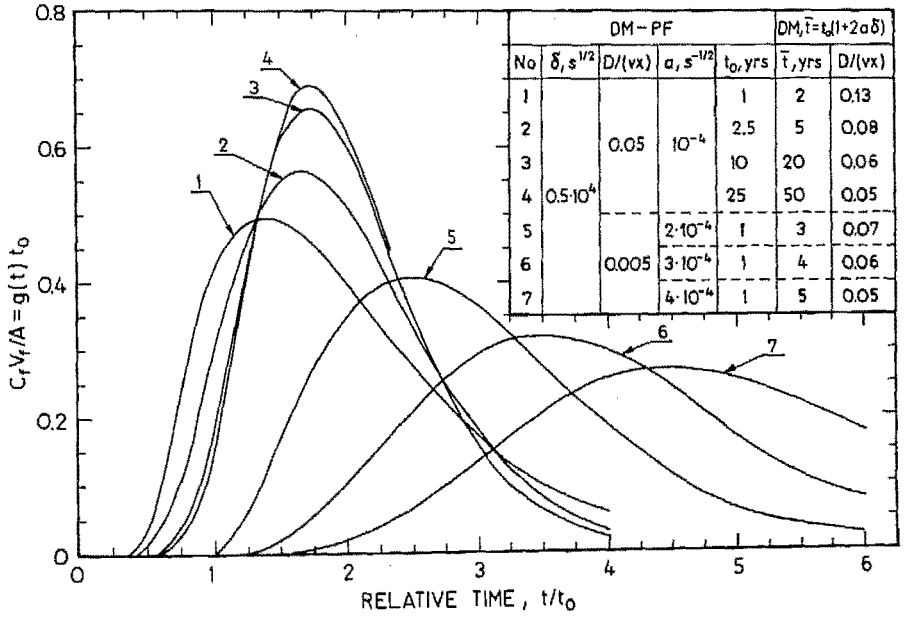

Fig. 5. Examples demonstrating that in long-term experiments the two-parameter ordinary dispersion model [eqn. (23)] transferred properly with the aid of eqn. (22), and eqn. (24) yields the same concentration curves as the four-parameter exact model [eqn. (5)].

may also be fitted; they will yield practically the same values of the parameters, if apparent (effective) $D/(vx)$ values are low (Kreft and Zuber, 1978).

One may wonder if the ordinary dispersion model is of any use at all. First of all, if an adequate tracer is utilized in the experiment, the parameters of the model, i.e., $\overline{t}_t$ and apparent Pe serve directly to predict the movement of pollutant. Another useful approximation may be derived from eqns. (22) and (10):

$$Q = V_f/t_o = RV_f/\overline{t}_t \tag{25}$$

If a non-adsorbable tracer is used, then from eqns. (21) and (22):

$$R = R_p \cong V_t/V_f \tag{26}$$

Putting eqn. (26) to (25) and dividing by the cross-section area one gets the expression for the Darcy velocity (v_f):

$$v_f = n_f v = n_f x/t_o = x(n_f + n_p)/\overline{t}_t \tag{27}$$

Equation (27) shows that the Darcy velocity can be estimated without knowledge of n_f, if $n_p \gg n_f$ and if n_p is known from core samples. Unfortunately, without an independent estimate of n_f, the real (interstitial) velocity remains unknown.

ENVIRONMENTAL RADIOISOTOPE TRACERS IN A STEADY STATE (e.g. ^{14}C)

The problem of interpretation of ^{14}C data was mentioned by Neretnieks (1981), and taken up by Małoszewski and Zuber (1983). Here a more general approach is given which somewhat extends the earlier findings. The solution for a continuous injection and a steady state is obtained by putting $C_f(0, t) = C_o$ instead of eqn. (3.2) and by finding the solution for $t \to \infty$ from:

$$\lim_{t \to \infty} C_f(x, t) = \lim_{s \to 0} s\overline{C}_f(x, s) \tag{28}$$

where $\overline{C}_f$ is the Laplace transform of C_f. For the dispersion model the solution is equivalent to eqn. (50) in Sudicky and Frind (1981), who dealt with contaminant transport. This solution seems to be inapplicable to the interpretation of tracer data. However, for a distant recharge area the piston flow model is an acceptable approximation for a steady-state input concentration. The solution for the piston flow is:

$$C_f(x)/C_o = \exp\{-\lambda t_o [1 + 2a\lambda^{-1/2} \tanh(\delta\lambda^{1/2})]\} \tag{29}$$

In eqn. (29) t_o is understood as a function of x according to eqn. (10). The radioisotope age, t_a, is defined by:

$$C_f/C_o = \exp(-\lambda t_a) \tag{30}$$

which is commonly used for calculating t_a from the experimental concentration values. Combining eqn. (30) with (29) one gets:

$$t_a/t_o = 1 + 2a\lambda^{-1/2}\tanh(\delta\lambda^{1/2}) \quad (31)$$

For $\delta\lambda^{1/2} \leqq 0.25$, eqn. (31) simplifies to:

$$t_a/t_o \cong 1 + 2a\delta \cong 1 + R_a n_p/n_f \quad (32)$$

since $\tanh(z) \cong z$ for $z \leqq 0.25$.

For $\delta\lambda^{1/2} \geqq 2$, eqn. (31) simplifies to:

$$t_a/t_o \cong 1 + 2a\delta\lambda^{-1/2} \quad (33)$$

since $\tanh(z) \cong 1$ for $z \geqq 2$.

Equation (31) and its simplified forms [eqns. (32) and (33)] show that the radiocarbon ages in fissured rocks with a porous matrix differ from the real ages of water (t_o). Consider the condition for the applicability of eqn. (32). After simple rearrangements and neglecting b in comparison with $L/2$ one gets:

$$L < 0.5(D_p/\lambda)^{1/2} = (2.55 \cdot 10^5 D_p^{1/2})_{^{14}C} \qquad (\text{for } D_p \text{ in m}^2\,\text{s}^{-1}) \quad (34)$$

which means that for ^{14}C and using D_p of the order of 10^{-10} m^2 s^{-1} any spacing not greater than 2.5 m satisfies eqn. (32). Thus, the approximation (32) is applicable under the most common conditions and will be used here to demonstrate some effects which may occur in ^{14}C dating. For a long confined aquifer with a constant water velocity the ^{14}C content along the distance from the recharge area may be expressed in terms of real age, because $t_o(x) = V/Q = x/v$. Assuming that the initial ^{14}C content (C_o) is well-known, the ^{14}C age [t_a from eqn. (30)] will be equal to t_o if there is no matrix porosity (Fig. 6A).

Consider now a nonradioactive tracer, i.e. the stable isotope composition of water molecules. There has been controversy over the reality of the stable isotope shift at the age of 10^4 yrs, i.e., at the change from the cold climate of the last Ice Age to the Holocene. The documented shift, compatible with ^{14}C ages shown theoretically in Fig. 6A, was presented by Blavoux and Olive (1981) for a sandy aquifer in France and by Ferronsky et al. (1983) for several aquifers in the Soviet Union. What will happen in a fissured aquifer with a porous matrix? For the values of parameters assumed in Fig. 6B both radioactive and nonradioactive tracers are delayed in the same way, because if eqn. (32) is applicable, there is no influence of λ on the retardation factor.

Imagine, now, that the fissure spacing is so large that $\delta\lambda^{1/2} = 2$, i.e. the radioactive tracer is not influenced by the presence of other fissures (approximate eqn. (33) which is equal to the exact solution for $L \to \infty$). However, the nonradioactive tracer moves with the mean velocity corresponding to eqn. (22) and thus the age determined from the stable isotope shift ($\delta^{18}O$ or δD) will differ from the ^{14}C age, as shown in Fig. 6C.

Following the work of Thilo and Münnich (1970), the possible adsorption (or exchange) of ^{14}C in fissured carbonate aquifers has commonly been neglected. The situation changes drastically if the matrix is characterized by

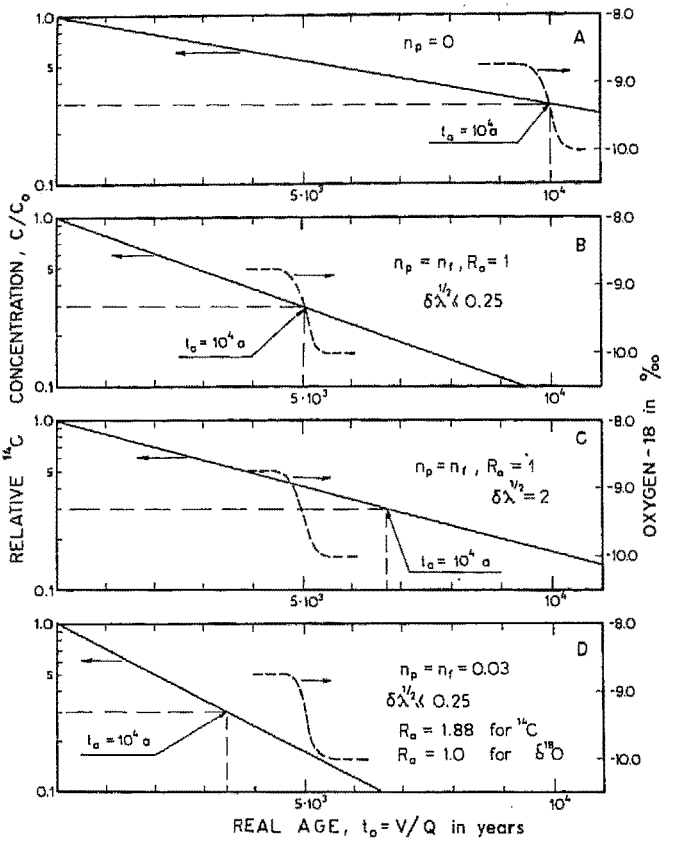

Fig. 6. Schematic presentation of the ^{14}C distribution and interpreted ages (t_a) as related to the real age (t_o). (A) no matrix diffusion, (B) matrix diffusion without adsorption, (C) as case (B) but with large fissure spacing yielding $\delta\lambda^{1/2} = 2$, (D) as case (B) but with some exchange ability of the rock material.

microporosity, which according to recent investigations is rather the rule than the exception (Neretnieks, 1980). Then even for a relatively low k_d value, equal to 0.05 $cm^3\ g^{-1}$, the adsorption retardation factor may be equal to about 1.9 (see the next section). In such a case the stable isotope shift, though delayed in respect to the real age, will occur much farther in the aquifer than the radioisotope age of 10^4 yrs (Fig. 6D). In an aquifer of a limited extent it may happen that the stable isotope shift has been completely lost, whereas the ^{14}C ages above 10^4 yrs are still preserved and observed. Now it becomes clear that some discrepancies observed in the past between the stable isotope data and ^{14}C ages were most probably caused by the effects explained in Fig. 6. Of the two methods, i.e. the stable isotope and ^{14}C, the former is to be trusted more, contrary to the common practice of the past. An even more important fact is that no radioisotope method can yield the real age of water unless the retardation factor is estimated independently.

THE ADSORPTION RETARDATION FACTOR

Equations (2), (2.1) and (13) are formulated for the concentration in the solid phase, commonly expressed in mass (or activity) of tracer per unit weight of the solid phase. Such a formulation is convenient for granular media to calculate R_a for a given granular material which may have different porosities (Inoue and Kaufman, 1962). For fissured media it is more logical to express the concentration in the solid phase as the mass of tracer adsorbed per unit rock surface, C_s'. Then the adsorption coefficient in the fissures is:

$$k_a = (C_s'/C_f)_{\text{equilibrium}} \tag{35}$$

and the retardation factor due to the adsorption in the fissures is:

$$R_{af} = 1 + Z_f k_a/n_f = 1 + k_a/b \tag{36}$$

where Z_f is the surface of fissure walls per unit volume of rock (Freeze and Cherry, 1979). Similarly, for the adsorption in the micropores, with a negligible adsorption in the fissures, the R_a factor is:

$$R_a = 1 + Z_p k_a/n_p \tag{37}$$

where Z_p is the ratio of the adsorption surface of the micropores to the unit rock volume and k_a is defined as (C_s'/C_p) at equilibrium, which of course is equal to eqn. (35).

A similar approach should be applied even to granular media, if the grain-size composition differs from that for which k_d was measured. Comparing eqn. (37), written down for a granular medium, with eqn. (13) one obtains the relationship between k_d and k_a for such a medium:

$$k_a = (1-n)\rho k_d/Z \tag{38}$$

where n is the porosity, and Z is the surface-to-volume ratio of the granular medium.

Assuming a spherical shape of the grains, the surface-to-volume ratio can be calculated from a known grain-size composition curve as follows: The grain-size curve is divided into j groups of weight fractions of ν_i. The number of spheres per unit rock volume in the ith group with the mean group radius, r_i, is:

$$\nu_i(1-n)\rho/[(4/3)\pi r_i^3]$$

and the surface-to-volume ratio of the ith group is:

$$4\pi r_i^2 \nu_i(1-n)\rho/[(4/3)\pi r_i^3]$$

The total surface-to-volume ratio of the spheres (Z_s) is the sum of the group ratios:

$$Z_s = 3(1-n)\sum_{i=1}^{j}(\nu_i/r_i) \tag{39}$$

Now, by putting eqn. (39) to (38) one obtains the relationship between k_d and k_a for a granular medium consisting of spheres:

$$k_a = (1/3)\rho k_d \sum_{i=1}^{j} (v_i/r_i) \tag{40}$$

Equations (38—40) show how k_d determined for ground rock material may be related to k_a, if one assumes that the adsorption on a freshly ground surface is the same as on an old surface. Having k_a from eqn. (40), or from a similar relationship for another grain shape, one can determine the retardation factor if Z_p (or Z_f in the case of $n_p = 0$) is known.

If the micropores can be approximated by a bunch of equal diameter capillaries, the Z_p factor is easily derived as:

$$Z_p = 4n_p/d_c \tag{41}$$

where d_c is the diameter of the capillary. The adsorption retardation factor is then:

$$R_a = 1 + 4k_a/d_c \tag{42}$$

if the absorption in fissures is negligible in comparison with the adsorption in the micropores. This assumption is undoubtedly well satisfied for $d_c \ll 2b$, as can be seen from comparison of eqn. (42) with (36).

Equations (39—42) are given to provide an estimate of k_a and R_a when no direct data exist. The adsorption surface of rock samples can be found from sorption of gases, whereas the dimensions of micropores are obtainable by electron microscopy observations. Neretnieks (1980) compiled some available data on the subject. However, the results of Thilo and Münnich (1970) indicate that the adsorption of gases does not yield correct retardation factors.

Consider an example. Assuming that a rock material with density 2.7 g cm^{-3} is ground to grains of 0.2 mm in diameter and that the k_d value measured in a bath experiment is 0.05 cm^3 g^{-1}, the adsorption retardation factor in that granular medium will be 1.20, if the porosity is 0.40 [eqn. (13)]. The k_a value from eqn. (40) is $4.4 \cdot 10^{-4}$ cm, and the R_{af} factor from eqn. (36) is then only 1.04 for the same material forming a hard rock with $n_p = 0$ and $2b = 0.2$ mm. However, in the case of $n_p \neq 0$ and micropores of 0.02 mm in diameter, the adsorption retardation factor will be 1.88, which means that even low k_d values yield high adsorption retardation in the case of a porous matrix. In this case, if $n_p = n_f$, then from eqn. (22) the total retardation factor will be equal to 2.88, as shown for ^{14}C in the example D of Fig. 6.

INTERPRETATION OF ARTIFICIAL TRACER EXPERIMENTS: CASE STUDIES

In this section several published tracer experiments will be interpreted to demonstrate the applicability of the models and their limitations in the

cases of limited knowledge of complementary parameters. All the examples considered are related to the two-well pulse method applied during the pumping tests. The flow is radial and the unidimensional approach is an approximation, generally considered to be satisfactory for practical purposes.

(a) Ivanovich and Smith (1978) described an experiment in the English Chalk, whereas Kreft and Zuber (1979) criticized their interpretation. It has appeared that none of the opponents were right after Glueckauf (1981) had reinterpreted the experiment taking into account the matrix diffusion. Here this experiment is recalled to demonstrate two models, i.e. the dispersion model of a single fracture (DM—SF) given by eqn. (15) and the piston flow model of a single fracture (PFM—SF) given by eqn. (17), as well as to show how other data can be utilized in the combined interpretation. The experimental data and the two fitted models are given in Fig. 7. As the DM—SF [eqn. (15)] is more exact than the PFM—SF [eqn. (17)], the parameters yielded by the former will be used in further considerations. These parameters are: $t_o = 1.5\,\mathrm{h}$, $a = 2.1 \cdot 10^{-2}\ \mathrm{s}^{-1/2}$, $D/u = 0.64\,\mathrm{m}$. The mean transit time of water, t_o, may serve for finding the fissure porosity utilizing data given in the afore cited works and neglecting the volume of the depression cone, which is justified in this case:

$$n_f = Q_p t_o/(\pi x^2 h) = 3.85 \cdot 1.5/(\pi 8^2 \cdot 13) = 0.0022 \qquad (43)$$

where Q_p is the pumping rate, x is the distance between the injection and pumping wells, and h is the thickness of the aquifer.

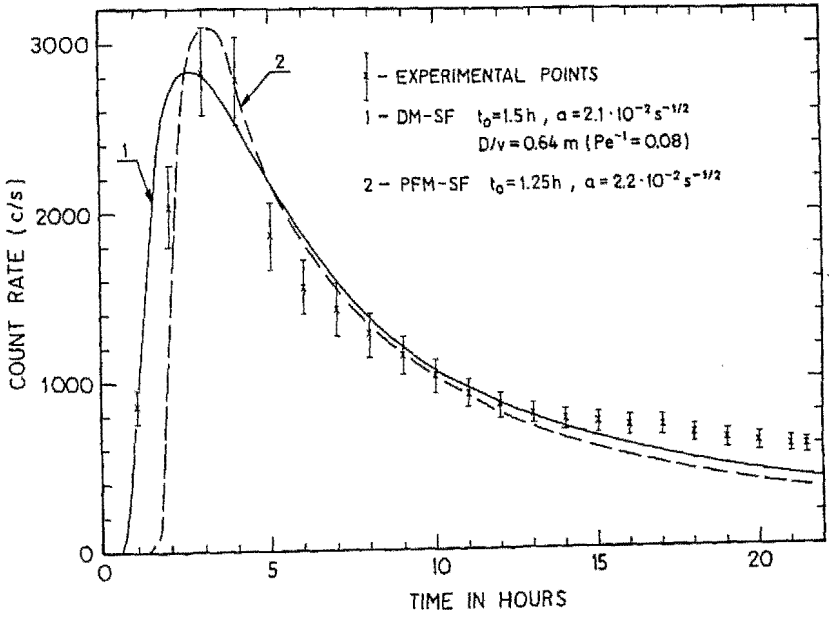

Fig. 7. Interpretation of a tracer experiment in the English Chalk. Experimental points after Ivanovich and Smith (1978). Curve 1 = eqn. (15), curve 2 = eqn. (17).

For the tortuous slits the following relation can be derived (Zuber, 1974):

$$K = n_f(2b)^2/(12\tau_f) \tag{44}$$

where K is the permeability coefficient and τ_f is the tortuosity coefficient of fissures defined as the relative lengthening of slits due to their tortuosity. Equation (44) can be rearranged to:

$$2b = \tau_f(k_{10}/n_f)^{1/2}/233 \tag{45}$$

where k_{10} is the hydraulic conductivity in m per day at 10°C and $2b$ in millimeters. For $k_{10} = 0.70$ m per day (Kreft and Zuber, 1979), $n_f = 0.0022$ from eqn. (43), and τ_f between 1.5 and 2.5, the fracture width is 0.11—0.19 mm.

The diffusion coefficient of tritium in the Chalk was estimated from the environmental tritium profile to be about 10^{-10} m^2 s^{-1} (Smith et al., 1970), which is in agreement with findings of Wellings (1984) who for the same formation gives $D_p \cong 0.1 D_m$, where D_m is the diffusion coefficient in free water. Taking $D_p = 10^{-10}$ m^2 s^{-1}, and $2b$ as above one can find the matrix porosity for the a-value determined from the tracer experiment (Fig.7) $n_p = a(2b)\sqrt{D_p} = 0.0206(0.11 \text{ to } 0.19)\cdot 10^{-3}/10^{-5} = 0.23$ to 0.39. This porosity is in agreement with the range of 0.15—0.40 reported by Foster (1975).

The piston flow model (Fig. 7) gives quite close values of parameters to those determined above whereas Glueckauf's parameters differ more, namely $t_o = 1$ h, $a = 0.025$ s$^{-1/2}$, and $D/v = 1.0$ m.

(b) Another experiment for the Chalk was performed according to Glueckauf (1981) by R. Bibby. The piston flow model, eqn. (17), fitted in Fig. 8, yielded $t_o = 1$ h and $a = 1.67\cdot 10^{-2}$ s$^{-1/2}$. For the matrix porosity range as above and for $D_p = 10^{-10}$ m^2 s^{-1} one gets $2b = 0.09$—0.24 mm, which is very close to the fracture widths found in the case (a) from n_f and k_{10} values. Again Glueckauf's interpretation was somewhat different. The next example yields much higher differences.

(c) Glueckauf (1981) also reported an experiment performed by R.G. Sun and J.B. Robertson in paleozoic fractured dolomite and limestone formations. The experimental points and the interpretation made with the aid of the PFM—SF are given in Fig. 9. The theoretical curve fitted to the initial part of the experiment yields a distinct second tracer path, which is also interpretable. Glueckauf obtained for the second curve a lower value of the a-parameter which suggests an unacceptable result, i.e. a wider fracture width. The interpretation presented here yields the second fissure width $a_1/a_2 = b_1/b_2 = 0.73$ times lower than the first one. As the flow velocity in fissures is proportional to b^3 (e.g. seen eqn. (3) in Grisak et al., 1980), the mean transit time of water should be $(0.73)^{-3} = 2.54$ times longer for the second path. Thus it should be $t_{o,2} = t_{o,1} \cdot 2.54 = 54$ h, which is in reasonable agreement with 65 h found directly.

(d) This example is taken from Kreft et al. (1974). A less step initial

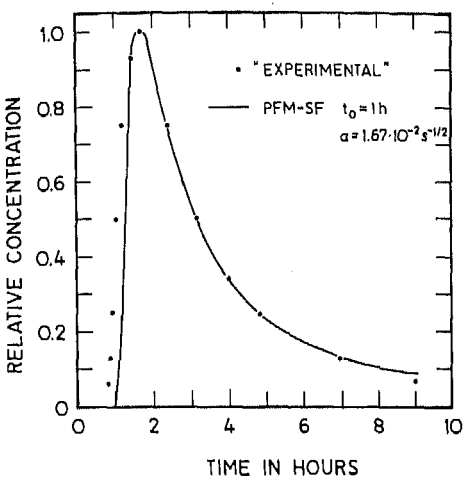

Fig. 8. Interpretation of a tracer experiment in the English Chalk. Experimental points according to Glueckauf (1981) after R. Bibby. Theoretical curve of eqn. (17).

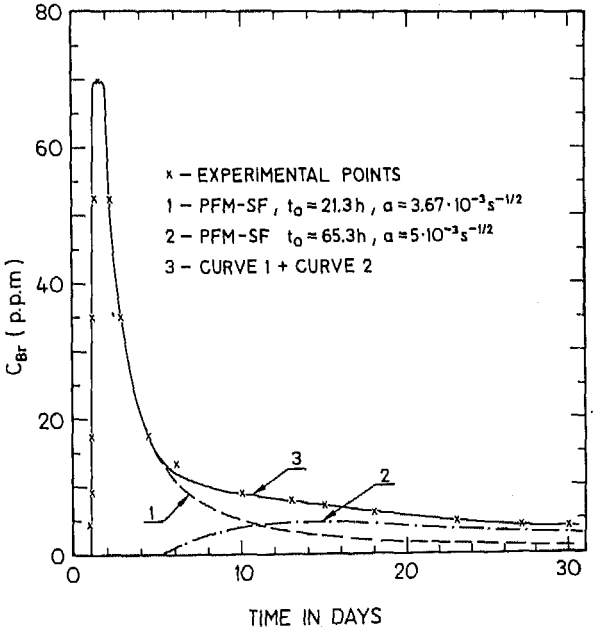

Fig. 9. Interpretation of a tracer experiment in fractured carbonate formation. Experimental points according to Glueckauf after R.G. Sun and J.B. Robertson. Theoretical curves of eqn. (17).

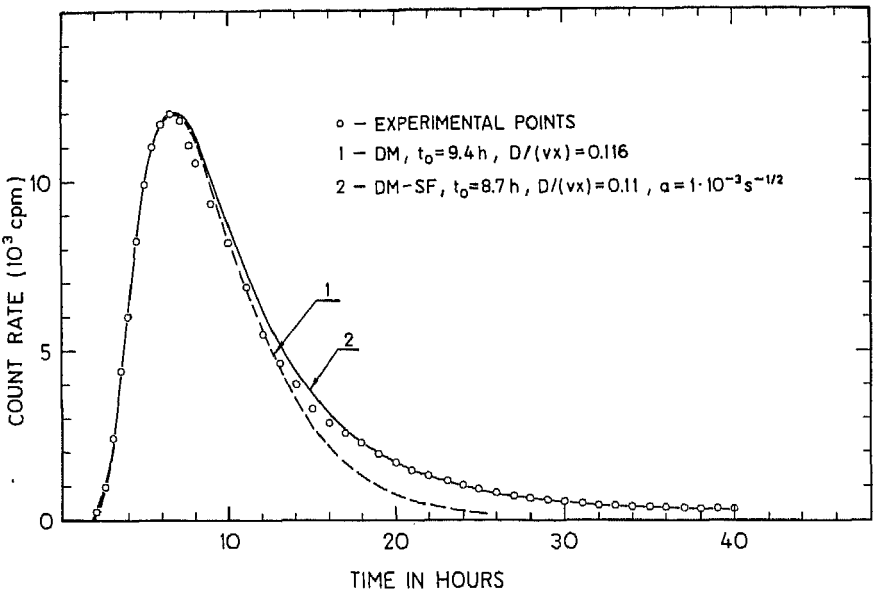

Fig. 10. Interpretation of a tracer experiment in a highly dispersive fractured dolomite. Experimental points after Kreft et al. (1974). Curve *1* = eqn. (23), curve *2* = eqn. (15).

part of the experimental curve (Fig. 10) than in the previous examples suggests a higher dispersivity and thus the dispersion model is unavoidable. The mean transit time of water, $t_o = 8.7$ h, yields from eqn. (43) the fissure porosity of 0.016. The hydraulic conductivity was 50 m per day (Zuber, 1974), which yields from eqn. (45) $2b = 0.24\tau_f$(mm). Assuming a reasonable value of D_p, i.e. 10^{-10} m^2 s^{-1}, and taking $a = 0.001\,s^{-1/2}$ from Fig. 10, one gets from eqn. (12), $n_p = 0.034$—0.058, for $\tau_f = 1.5$—2.5, respectively.

The obtained matrix porosity agrees reasonably well with the mean value of $n_p = 0.064$ found by J. Motyka (pers. commun., 1984) for core samples of the same formation taken from a well at a distance of ~ 2 km.

As already mentioned the dispersivity in this example is much higher than in the previous examples. The ordinary dispersion model, eqn. (23), yields both t_o and D/v close to the values of the exact model (Fig. 10). The original interpretation of Kreft et al. (1974) in which the tail was interpreted as another flow path has to be rejected in view of the theory presented here.

(e) This example is taken from Lenda and Zuber (1970). The PFM—SF gives somewhat worse fitting than the DM—SF (Fig. 11). The t_o parameter of the former yields $n_f = 6 \cdot 10^{-4}$ (for $x = 22$ m, $h = 57$ m, and $Q_p = 1.73$ m^3 min^{-1}). This n_f value for the known $k_{10} = 41$ m per day gives $2b = 1.12\,\tau_f$ (mm) and for $a = 0.064\,s^{-1/2}$, and assuming $D_p = 10^{-10}$ m^2 s^{-1}, one gets quite an improbable value of $n_p = 7.16\tau_f$. On the other hand the dispersion model (DM—SF) yields reasonable values of parameters, i.e. $n_f = 3.5 \cdot 10^{-2}$, $2b = 0.15\tau_f$(mm), and $n_p = 0.047\tau_f$. The accuracy of these figures is rather

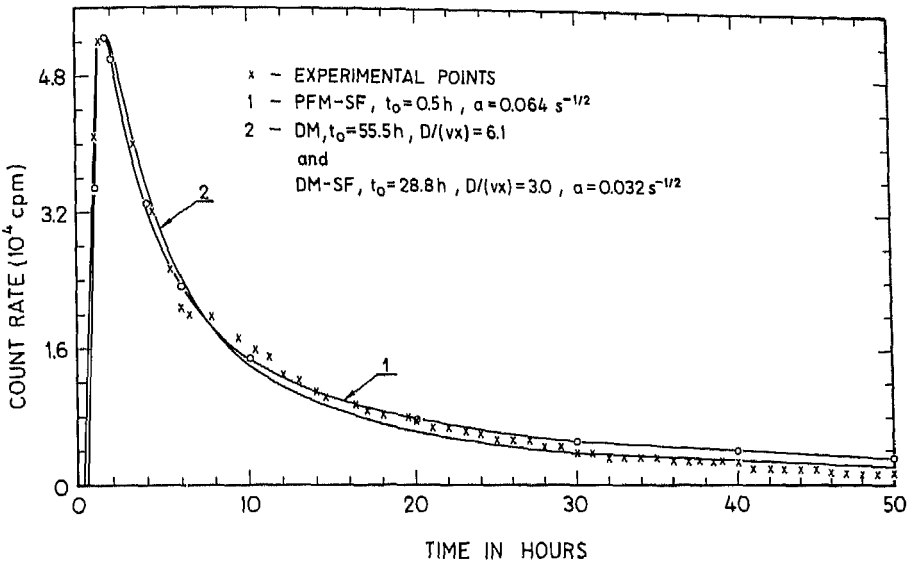

Fig. 11. Interpretation of a tracer experiment in an extremely dispersive fractured dolomite. Experimental points after Lenda and Zuber (1970). Curve *1* = eqn. (17), curve *2* = eqn. (15) and also eqn. (23) with transformations (22) and (24).

low as discussed later, but nevertheless in the authors' opinion they are more probable than any of the values reported for this well (pumping well No. PS-9, observation wells No. PS-9a and PS-10) in Wilk and Motyka (1980). An unusually complex geological situation (see fig. 1 in Kreft et al., 1974) makes the results of pumping tests very doubtful. Because of a high dispersivity the tracer experiment also yields parameters of limited accuracy. The interpretation of Kreft et al. (1974), made with the aid of the automatically fitting computer program of Kreft and Lenda (1974), showed that in the cases of extremely high values of the $D/(vx)$ parameter, the results are not unambiguous. Zuber (1983) presented some quantitative results obtained by A. Kreft who proved that due to measuring errors an interplay of parameters occurs and consequently different pairs of t_0 and $D/(vx)$ yield curves which give practically the same fit to the experimental data. The same is probably also true for the three-parameter model of eqn. (15) although this model yields a lower dispersivity. Thus the obtained values of parameters are of low accuracy.

It should be added that examples (d) and (e) represent the only two smooth curves obtained in a number of measurements performed in the same geological formation. Other measurements yielded curves with more than one peak (most interesting examples can be found in Zuber, 1983) and their reinterpretation is still to be done. The reinterpretation of (d) and (e) presented here shows that the originally interpreted dispersivities (2.1 and 110 m, respectively) were undoubtedly too high (apparent values).

However, even if the matrix diffusion is taken into account, both examples still yield relatively high dispersivity which is related to the heterogeneity of the system, as proved by peaked curves in other experiments.

(f) The last example is related to the case of a simultaneous use of a non-adsorbable tracer ($R_a = 1$) and an adsorbable one ($R_a > 1$). The measurement of Landström et al. (1978) was originally interpreted with the aid of eqn. (23). Glueckauf (1981) tried to reinterpret this measurement reaching a conclusion that "the two evaluations are simply not compatible with our theory". Here it will be shown that they are compatible with the theory developed within this paper. Figure 12 demonstrates two concentration curves obtained with ^{82}Br and ^{85}Sr tracers applied in a fracture granite. Both curves yield the same t_o and are thus compatible.

The experiment did not satisfy the conditions necessary for a proper interpretation of n_f from the combined tracer and pumping data (Zuber, 1974). However, some other information can be extracted as shown below. Namely, Landström et al. (1978) report the $k_d = 1.5\ cm^3\ g^{-1}$ measured in a batch experiment with dried drill cuttings of known grain-size composition. From their data applied to eqn. (40) one gets $k_a = 0.0076$ cm. This k_a value together with $R_a = 11.5$ found in Fig. 12 yields from eqn. (42) $d_c = 29\ \mu m$ as the diameter of micropores. Assuming, on the other hand, $n_p = 0.02$ and $D_p = 10^{-10}\ m^2\ s^{-1}$, and taking a_1 from Fig. 12 one gets from eqn. (12) $2b = 56\ \mu m$ as the fracture width. The close value of the diameter of the micropores to the fracture widths is surprising, although it is possible. However, it may be suspected that the freshly ground material yielded higher k_a value than the real in-situ value. Thus, d_c found from eqn. (42) is rather too high. Of course, for a proper interpretation, the n_p, d_c, and D_p parameters should be known from laboratory measurements. The figures

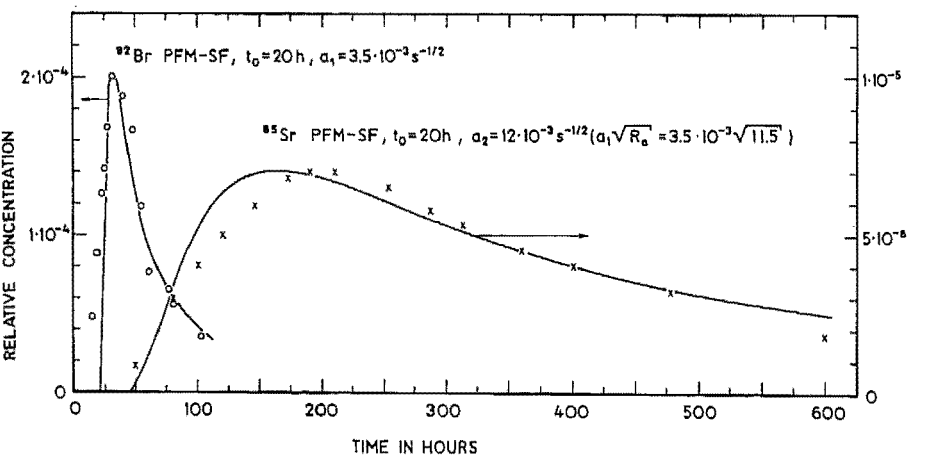

Fig. 12. Experimental points after Landström et al. (1978), theoretical curves of eqn. (17).

given above are far from exact, but they show that the parameters obtained from the fitting in Fig. 12 (i.e. a_1 and R_a) yield reasonable orders of magnitudes of other related parameters.

INTERPRETATION OF ENVIRONMENTAL TRACER DATA: CASE STUDY

As mentioned earlier any mathematical model utilized for the interpretation of environmental tracer data will yield the mean age of tracer (the mean exit age, or the mean transit time of tracer). This physical quantity may be of interest when a regional pollution hazard is considered. For other purposes the real age of water is sought. Blavoux and Olive (1981) described the ^{14}C and stable isotope study of a large sandy aquifer in France. As there was no double porosity the ^{14}C age represented the real age and agreed more or less with the stable isotope shift, which confirms the idea presented in Fig. 6A.

Fontes and Garnier (1979) described the environmental tracer study of the confined aquifer of the "calcaires carbonifères" in northern France and Belgium. Two samples yielded ages greater than 10,000 yrs but there was no stable isotope shift. According to table 6 of that work, the groundwater velocities determined from the ^{14}C data, denoted here as v_t, are on average about 2.7 times lower than the Darcy velocities v_f, although they should be n_f^{-1} times higher. This means that if $n_f = 0.01$ the velocity determined from ^{14}C is about 270 times lower than the groundwater velocity known from conventional data. Fontes and Garnier were unable to offer an explanation of this surprising result. The model developed here offers a possible explanation. Namely, eqn. (22) can be rewritten as $v = (1 + n_p R_a / n_f) v_t$. By inserting $v_f = n_f v$, rearranging, and simplifying one gets:

$$v_f / v_t \cong R_a n_p \tag{46}$$

which shows that for $v_f / v_t = 2.7$, the R_a factor must be at least about 20 to get any reasonable n_p value. Is such a value of R_a possible at all for ^{14}C in a carbonate aquifer? To answer this question the classic work of Thilo and Münnich (1970) has to be recalled. In their table I laboratory column experiments are reported. Among other experiments, the delay of ^{14}C in the form of $H^{14}CO_3^-$ was measured in ground limestone material of the grain diameter 90 μm. Seven runs yielded the average adsorption retardation factor, $R_a = 2.8$. This value inserted to eqn. (37), formulated for a granular medium and with eqn. (39) for the specific surface, leads to $k_a = 81$ μm. If it is additionally assumed that the micropore diameter (d_c) is equal to 10 μm, one gets from eqn. (42) the adsorption retardation factor $R_a = 32.4$. Putting this R_a value into eqn. (46) yields somewhat high but still reasonable matrix porosity, $n_p = 0.08$. It is difficult to say how far these speculations are true. The real k_a value may differ from that taken from Thilo and Münnich, just as the real d_c may differ from the one assumed. Consequently, the calculated n_p

value may also differ from the true value. However there is no doubt that the matrix diffusion and ^{14}C exchange are the main processes responsible for the delay of ^{14}C, which in this case is of the order of two magnitudes.

It is worth mentioning that if n_f is assumed to be about 0.01, then for $k_{10} = 1.73$ m per day, taken from Fontes and Garnier (1979), one gets from eqn. (45) $2b = \tau_f \cdot 0.056$ mm = 84—140 μm. This lower value together with $k_a = 81\,\mu$m found above yields from eqn. (36) $R_{af} \cong 2$, which means that in the case of carbonate rocks of low permeability (narrow fissures) the retardation in fissures is not negligible even if $n_p = 0$.

All these findings are in sharp contrast with the conclusions reached by Thilo and Münnich (1970). However, these authors were unable to take into account the microporosity effects because at that time the existence of microporosity in most rock materials and its importance were unknown.

CONCLUSIONS

Analytical solutions have been obtained for the problem of tracer movement in parallel fractures. The exact solution (5) contains four parameters. Numerical calculations show that in long-term (a few years) tracer experiments the tracer moves as if the movement were in the whole water volume, i.e. both in fissures and in micropores of the matrix. The number of parameters may then be reduced to two as the ordinary dispersion model [eqn. (23) with (22) and (24)] provides the mean transit time of tracer which is related to the mean transit time of water by the retardation factor [eqn. (20)], which has to be determined independently.

In short-term experiments (tens of hours), the tracer movement is not affected by the fissure spacing, and the single fissure approximations are applicable [eqn. (15) or (17)]. If the dispersivity is low, a very simple, two-parameter formula [eqn. (17)] is applicable. In the case of high dispersivity the use of the dispersion model [eqn. (15)] becomes necessary, and the number of fitting parameters increases to three (t_o, a and D/vx). In some cases, if both the a-parameter and the dispersivity (D/v) are low, the ordinary dispersion model [eqn. (23)] is also applicable as a rough approximation but then the information on matrix diffusion is lost.

In intermediate-term tracer experiments (several months) no approximation is possible, with the exception of the cases with a high a-value, where the dispersivity is negligible.

A number of artificial tracer experiments have been interpreted with the aid of derived formulae. Relatively good fittings have been obtained in all the cases, and the values of parameters agree reasonably well with the information available. Considering all the approximating assumptions (parallel fissures of equal fracture width and spacing) the model seems to work very well. In the case of a high dispersivity, the unambiguous fitting is not possible. However, if some knowledge of parameters is available a proper model

selection is easier. In general, such parameters as matrix porosity and the coefficient of matrix diffusion (measurable on core samples), as well as the hydraulic conductivity (known from pumping tests) are helpful in the interpretation. In the cases of adsorbable tracers the dimensions of micropores (or microfissures) measurable by microscope observations of core samples and the distribution coefficient measurable in batch or column experiments of ground material should also be very helpful.

Considerations related to the environmental ^{14}C show that no tracer can yield a real age of water if the retardation factor is not determined independently. In the case of ^{14}C ages in carbonate fissured rocks a discrepancy may exist between the ^{14}C ages and the stable isotope shift caused by climatic changes at the end of the last glaciation. This discrepancy is caused by the possible adsorption (exchange) of ^{14}C in the porous matrix, which is not as negligible as was thought, when the microporosity was not considered to be an important parameter. In the past, too much weight was put to the ^{14}C method, whereas more weight should be attributed to the stable isotope method.

Further studies are certainly needed to develop more realistic models which would take into account unequal spacing and lognormal distributed fissure aperture. However, the present study indicates that in short-term experiments the fissure spacing does not influence the tracer distribution, thus it is of little importance whether it is regular or not. On the other hand, in long-term experiments the tracer is homogeneously distributed as if the movement was taking place in the whole water volume, thus again the fissure spacing has no influence. The problem remains to be solved for intermediate-term experiments and for unequal fissure aperture. However, the effective fissure apertures estimated in this work from the pumping tests seem to yield realistic matrix porosities when utilized in the a-parameter. Thus, it may be concluded that the model developed is applicable for practical purposes, in spite of its approximate nature.

ACKNOWLEDGEMENTS

A part of this study was performed during the stay of one of the authors (P.M.) at the Institute for Radiohydrometry, GSF, Neuherberg, financed by the Technical University of Braunschweig, W. Germany.

NOTATION

List of symbols used

A	injected mass or activity	M
A_o	$= A/(n_f v S)$	$M L^{-3} T$
a	fitting parameter defined by eqn. (12)	$T^{-1/2}$
b	half-fissure aperture	L
C_f	tracer concentration in water in the fissures	$M L^{-3}$

C_o	constant input concentration	$M\,L^{-3}$
C_p	tracer concentration in water in the matrix	$M\,L^{-3}$
C_s	tracer concentration in the solid phase expressed as mass of tracer per unit mass of rock, dimensionless	
C_s'	tracer concentration in the solid phase expressed as mass of tracer per unit rock surface	$M\,L^{-2}$
D	dispersion coefficient in the fissures	$L^2\,T^{-1}$
D_p	molecular diffusion coefficient in the porous matrix	$L^2\,T^{-1}$
D/v	dispersivity	L
$D/(vx)$	dispersion parameter, dimensionless	
d_c	diameter of the microcapillary	L
$g(t)$	weighting function (exit age distribution)	T^{-1}
h	aquifer thickness	L
K	permeability coefficient	L^2
k_a	adsorption coefficient defined by eqn. (35)	L
k_d	distribution coefficient, $k_d = C_s/C_p$	$L^3\,M^{-1}$
k_{10}	hydraulic conductivity in m per day at 10°C	$L\,T^{-1}$
L	fissure spacing	L
n	porosity, dimensionless	
n_f	fissure porosity, dimensionless	
n_p	matrix porosity, dimensionless	
Pe	Pêclet number, i.e. the reciprocal of the dispersion parameter, dimensionless	
Q	volumetric flow rate through the system	$L^3\,T^{-1}$
Q_p	volumetric pumping rate	$L^3\,T^{-1}$
R	total retardation factor, dimensionless	
R_a	retardation factor due to the adsorption in the matrix, dimensionless	
R_{af}	retardation factor due to the adsorption in the fissures, dimensionless	
R_p	retardation factor due to the diffusion into a porous matrix, dimensionless	
r_i	mean grain radius in the ith group	L
S	cross-section area perpendicular to flow	L^2
t	time variable	T
t_a	radioisotope age, defined by eqn. (30)	T
$\bar{t}_o$	mean transit time of water defined by eqn. (10)	T
$\bar{t}_t$	mean transit time of tracer defined by eqn. (18)	T
V_f	volume of water in fissures, i.e. mobile water volume	L^3
V_t	total volume of water in the system	L^3
v	mean water velocity in fissures, defined as $n_f v_f$	$L\,T^{-1}$
v_f	Darcy velocity defined as Q/S	$L\,T^{-1}$
v_t	mean tracer velocity defined as $x/\bar{t}_t$	$L\,T^{-1}$
x	spatial coordinate taken in the direction of flow	L
y	spatial coordinate perpendicular to the fissures extension	L
Z	surface-to-volume ratio for a granular medium i.e. the total surface of rock per unit volume	L^{-1}
Z_f	surface-to-volume ratio for a fissured medium	L^{-1}
Z_p	surface-to-volume ratio for the microporous matrix	L^{-1}
Z_s	surface-to-volume ratio for spheres	L^{-1}
δ	fitting parameter defined by eqn. (11)	$T^{1/2}$
λ	decay constant	T^{-1}
ν_i	weight fraction of the ith group of grains, dimensionless	
ρ	density of matrix material	$M\,L^{-3}$
τ_f	tortuosity factor for fissures, dimensionless	

REFERENCES

Barker, J.A., 1982. Laplace transform solutions for solute transport in fissured aquifers. Adv. Water Resour., 6: 98—104.

Barker, J.A., 1985. Block-geometry functions characterizing transport in densely fissured media. J. Hydrol., 77: 263—279.

Black, J.H. and Kipp Jr., K.L., 1983. Movement of tracers through dual-porosity media — Experiments and modelling in the Cretaceous Chalk, England. J. Hydrol., 62: 287—312.

Blavoux, B. and Olive, Ph., 1981. Radiocarbon dating of groundwater of the aquifer confined in the Lower Triassic sandstones of the Lorraine region, France. J. Hydrol., 54: 167—183.

Colville, J.S., 1984. Estimation of aquifer recharge and flow from natural tritium content of groundwater. J. Hydrol., 67: 195—222.

Ferronsky, V.I., Vlasova, L.S., Esikov, A.D., Polyakov, V.A., Seletsky, Yu.B., Punning, Ya.M.K. and Vajkuyaech, R.A., 1983. Relationship between climatic changes and variations in isotopic composition of groundwater, precipitation and organic soil matter in the Quaternary period. In: Paleoclimates and Paleowaters: A Collection of Environmental Isotope Studies. Int. At. Energy Agency (I.A.E.A.), Vienna, pp. 13—35.

Fontes, J.C. and Garnier, J.M., 1979. Determination of the initial ^{14}C activity of the total dissolved carbon: a review of the existing models and a new approach. Water Resour. Res., 15: 399—413.

Foster, S.S.D., 1975. The Chalk groundwater tritium anomaly — a possible explanation. J. Hydrol., 25: 159—165.

Freeze, J.A. and Cherry, J.F., 1979. Groundwater. Prentice-Hall, Englewood Cliffs, N.J.

Glueckauf, E., 1981. The movement of solutes through aqueous fissures in micorporous rock during borehole experiments. UKAEA Rep. AERE-R-10043.

Grisak, G.E. and Pickens, J.F., 1980. Solute transport through fractured media, 1. The effect of matrix diffusion. Water Resour. Res., 16: 719—730.

Grisak, G.E. and Pickens, J.F., 1981. An analytical solution for solute transport through fractured media with matrix diffusion. J. Hydrol., 52: 47—57.

Grisak, G.E., Pickens, J.F. and Cherry, J.A., 1980. Solute transport through fractured media, 2. Column study of fractured till. Water Resour. Res., 16: 731—739.

Inoue, Y. and Kaufman, W.J., 1962. Prediction of movement of radionuclides in solution through porous media. Health Phys., 9: 705—715.

Ivanovich, M. and Smith, D.B., 1978. Determination of aquifer parameters by a two-well pulsed method using radioactive tracers. J. Hydrol., 36: 35—45.

Kreft, A. and Lenda, A., 1974. A Fortran program for the interpretation of porosity measurements by the two-well pulse technique. Inst. of Nuclear Physics and Techniques, Rep. INT 46/I, Cracow.

Kreft, A. and Zuber, A., 1978. On the physical meaning of the dispersion equation and its solutions for different initial and boundary conditions. Chem. Eng. Sci., 33: 1471—1480.

Kreft, A. and Zuber, A., 1979. Determination of aquifer parameters by a two-well pulsed method using radioactive tracers — Comments. J. Hydrol., 41: 171—176.

Kreft, A., Lenda, A., Turek, B., Zuber, A. and Czauderna, K., 1974. Determination of effective porosities by the two-well pulse method. In: Isotope Techniques In Groundwater Hydrology 1974. Int. At. Energy Agency (I.A.E.A.), Vienna, pp. 295—312.

Landström, O., Klockars, C.E., Holmberg, K.E. and Westerberg, S., 1978. In situ experiments on nuclide migration in fractured crystalline rocks. Kärn-bränsle-säkerhet Technisk Rapport 110, Stockholm.

Lenda, A. and Zuber, A., 1970. Tracer dispersion in groundwater experiments. In: Isotope Hydrology 1970. Int. At. Energy Agency (I.A.E.A.), Vienna, pp. 619—641.

Małoszewski, P. and Zuber, A., 1982. Determining the turnover time of groundwater systems with the aid of environmental tracers, 1. Models and their applicability. J. Hydrol., 57: 207—231.

Małoszewski, P. and Zuber, A., 1983. Interpretation of artificial and environmental tracers in fissured rocks with a porous matrix. In: Isotope Hydrology 1983. Int. At. Energy Agency (I.A.E.A.), Vienna, pp. 635—651.

Neretnieks, I., 1980. Diffusion in the rock matrix. An important factor in radionuclide retardation? J. Geophys. Res., 85 (B8): 4379—4397.

Neretnieks, I., 1981. Age dating of groundwater in fissured rock: Influence of water volume in micropores. Water Resour. Res., 17: 421—422.

Neretnieks, I., Eriksen, T. and Tähtinen, P., 1982. Tracer movement in a single fissure in granitic rock: Some experimental results and their interpretation. Water Resour. Res., 18: 849—858.

Rasmuson, A. and Neretnieks, I., 1981. Migration of radionuclides in fissured rock: The influence of micropore diffusion and longitudinal dispersion. J. Geophys. Res., 86(B5): 3749—3758.

Smith, D.B., Wearn, P.L., Richards, H.J. and Rowe, P.C., 1970. Water movement in the unsaturated zone of high and low permeability strata by measuring natural tritium. In: Isotope Hydrology 1970. Int. At. Energy Agency (I.A.E.A.), Vienna, pp. 73—87.

Sudicky, E.A. and Frind, E.O., 1981. Carbon 14 dating of groundwater in confined aquifers: Implications of aquitard diffusion. Water Resour. Res., 17: 1060—1064.

Sudicky, E.A. and Frind, E.O., 1982. Contaminant transport in fractured porous media: Analytical solutions for a system of parallel fractures. Water Resour. Res., 18: 1634—1642.

Tang, D.H., Frind, E.O. and Sudicky, E.A., 1981. Contaminant transport in fractured porous media: Analytical solution for a single fracture. Water Resour. Res., 17: 555—564.

Thilo, L. and Münnich, K.O., 1970. Reliability of ^{14}C dating of groundwater in view of carbonate exchange. In: Isotope Hydrology 1970. Int. At. Energy Agency (I.A.E.A.), Vienna, pp. 259—270.

Wellings, S.R., 1984. Recharge of the Upper Chalk aquifer at a site in Hampshire, England, 2. Solute movement. J. Hydrol., 69: 275—286.

Wilk, Z. and Motyka, J., 1980. Groundwater storativity of karst fissured Triassic rocks in the eastern section of the Cracow-Silesian monocline. Ann. Soc. Geol. Pologne, 50: 447—484.

Zuber, A., 1974. Theoretical possibilities of the two-well pulse method. In: Isotope Techniques in Groundwater Hydrology, 1974. Int. At. Energy Agency (I.A.E.A.), Vienna, pp. 277—294.

Zuber, A., 1983. Models for tracer flow. In: Tracer Methods in Isotope Hydrology. Int. At. Energy Agency (I.A.E.A.), report TECDOD-291, Vienna, pp. 67—112.

Zuber, A., 1985. Mathematical models for the interpretation of environmental radioisotopes in groundwater systems. In: P. Fritz and J.CH. Fontes (Editors), Handbook of Environmental Isotope Geochemistry, Vol. 2. Elsevier, Amsterdam, pp. 1—60.